Distribution Agreement

In presenting this thesis or dissertation as a partial fulfillment of the requirements for an advanced degree from Emory University, I hereby grant to Emory University and its agents the non-exclusive license to archive, make accessible, and display my thesis or dissertation in whole or in part in all forms of media, now or hereafter known, including display on the world wide web. I understand that I may select some access restrictions as part of the online submission of this thesis or dissertation. I retain all ownership rights to the copyright of the thesis or dissertation. I also retain the right to use in future works (such as articles or books) all or part of this thesis or dissertation.

| Signature: | |
|----------------------|----------|
| Stephanie M. Garceau | Date |

Identifying the Genetic Drivers of 3q29 Deletion-Associated Phenotypes

Ву

Stephanie M. Garceau Master of Science

Graduate Division of Biological and Biomedical Science Genetics and Molecular Biology

| Tamara Caspary, Ph.D. |
|---|
| Advisor |
| |
| |
| |
| Androw Eggova Dh D |
| Andrew Escayg, Ph.D. |
| Committee Member |
| |
| |
| |
| Jennifer G. Mulle, Ph.D. |
| Committee Member |
| Committee Member |
| |
| |
| |
| |
| |
| A4- 1. |
| Accepted: |
| |
| |
| Lisa A. Tedesco, Ph.D. |
| Dean of the James T. Laney School of Graduate Studies |
| 2 can of the values 1. Laney Senson of Graduite Studies |
| |
| |
| Date |

By

Stephanie M. Garceau B.A., Communication, University of Minnesota Duluth, 2016 B.S., Cell and Molecular Biology, University of Minnesota Duluth, 2016

Advisor: Tamara Caspary, Ph.D.

An abstract of
A thesis submitted to the Faculty of the
James T. Laney School of Graduate Studies of Emory University
in partial fulfillment of the requirements for the degree of
Master of Science
in Graduate Division of Biological and Biomedical Science
Genetics and Molecular Biology
2019

Abstract

Identifying the Genetic Drivers of 3q29 Deletion-Associated Phenotypes

By Stephanie M. Garceau

The 3q29 deletion is a 1.6 Mb, heterozygous deletion that confers a greater than 40-fold increased risk for schizophrenia. This deletion also confers increased risk for other neurodevelopmental disorders, including autism spectrum disorder and intellectual disability. To interrogate the biological consequences of the 3q29 deletion, the Emory 3q29 project mouse team generated a mouse model harboring a heterozygous deletion of the syntenic region on mouse chromosome 16. These mice display social interaction and growth deficits similar to phenotypes observed in humans with the 3q29 deletion. The FVB mouse genetic background altered the observed growth deficits suggesting that genetic background can modulate the genotype-phenotype relationship. Given the attention that DLG1 has received as a candidate gene, we used $Dlg1^{+/-}$ mice to determine if DLG1 is the causal gene for the observed phenotypes. We saw minor growth deficits in the $Dlg^{+/-}$ mice but did not observe behavioral deficits. To narrow the critical region of distinct phenotypes identified in the full deletion mice, I used CRISPR/cas9 to generate two additional mouse models harboring heterozygous sub deletions of the 3q29 interval. Taken together, we show that the 3q29 deletion mouse model is a tractable entry point to understanding the biological mechanisms underlying complex deletion-associated phenotypes, including neurodevelopment disorders.

By

Stephanie M. Garceau B.A., Communication, University of Minnesota Duluth, 2016 B.S., Cell and Molecular Biology, University of Minnesota Duluth, 2016

Advisor: Tamara Caspary, Ph.D.

A thesis submitted to the Faculty of the
James T. Laney School of Graduate Studies of Emory University
in partial fulfillment of the requirements for the degree of
Master of Science
in Graduate Division of Biological and Biomedical Science
Genetics and Molecular Biology
2019

This thesis is adapted from the following published manuscript on which I am an author:

Rutkowski, TP, Purcell, RH, Pollak RM, **Grewenow**, **SM**, Gafford, GM, Malone, T, Khan, UA, Schroeder, JP, Epstein, MP, Bassell, GJ, Warren, ST, Weinshenker, D, Caspary, T, Mulle, JG. 2019. "Behavioral changes and growth deficits in a CRISPR engineered mouse model of the schizophrenia-associated 3q29 deletion." Molecular Psychiatry. PMID 30976085

| Introduction | 1 |
|--------------|----|
| Methods | 9 |
| Results | 14 |
| Discussion | 20 |
| Table 1 | 27 |
| Table 2 | 28 |
| Table 3 | 29 |
| Figure 1 | 30 |
| Figure 2 | 31 |
| Figure 3 | 32 |
| Figure 4 | 33 |
| Figure 5 | 34 |
| Figure 6 | 35 |
| References | 36 |

Introduction

Neurodevelopmental disorders, such as autism spectrum disorder, intellectual disability, and schizophrenia, are characterized by alterations in cognitive function. Twin studies identify a substantial heritable component for neurodevelopmental disorders. ^{1,2} The estimated heritability of schizophrenia and autism is 81% and 90% respectively.^{3,4} Although the heritability of these disorders is clear, the underlying genetic drivers remain elusive. Efforts to detect risk loci for neurodevelopmental conditions using linkage studies have been largely unsuccessful.⁵ These findings, or lack thereof, support the idea that these complex conditions are not driven by highly penetrant mutations at one, or even a few, genes. Candidate gene by environment interaction studies attempt to define how genetic and environmental factors contribute to overall disease risk. These studies require prior knowledge to identify causal candidates and are typically underpowered which limits their success. Genome-wide association studies (GWAS) of neurodevelopmental disorders leverage large sample sizes to reveal common genetic risk loci that confer minimal increases in risk. A GWAS with almost 37,000 schizophrenia cases and over 113,000 controls finds 108 risk loci. 8 Identification of numerous risk loci in GWAS suggest that complex phenotypes, like neurodevelopmental disorders, are polygenic in nature. Collectively, common variants confer substantial risk for neurodevelopmental disorders, but individually their effects are weak and variable. Recent findings identify a class of rare variants that individually have a stronger effect on risk, termed copy number variants.

Copy number variants (CNV) are large, typically >1kb, duplications or deletions of the genome. Intervals susceptible to alterations in copy number are flanked by segmental duplications, or low copy repeats, that are the substrate for nonallelic homologous recombination. Pathogenic CNVs are rare, highly penetrant genomic alterations implicated in

neurodevelopmental disorders. 9 Individual CNVs confer substantial increased risk for neurodevelopmental disorders, like schizophrenia, providing a genetic entry point for understanding these complex conditions. ¹⁰ Early studies identify genomic disorders that arise from de novo CNVs and display low phenotypic variability with high penetrance of characteristic phenotypes. 11 For example, individuals with Smith-Magenis Syndrome harbor a chromosomal deletion at 17p11.2 and have a distinct phenotypic profile including facial dysmorphisms, intellectual disability, and sleep disturbances. ¹² An additional category of pathogenic CNVs associated with neurodevelopmental disorders are those with variable phenotypic expressivity. 11 The 22q11.2 deletion is the most common pathogenic CNV occurring 1 in 4,000 live births. 13 The clinical profile of the 22q11.2 deletion includes increased risk for other neurodevelopmental disorders including intellectual disability and autism spectrum disorder accompanied by distinguishing physical anomalies. ¹⁴ Most notably, the 22q11.2 deletion has been identified as one of the largest known genetic risk factors for schizophrenia.¹⁵ The only other known CNV that confers comparable risk for schizophrenia is the 3q29 deletion. 15,16

The 3q29 deletion is a 1.6 megabase (Mb), heterozygous deletion on the long arm of chromosome 3. Most of the reported cases of 3q29 deletion syndrome are recurrent, *de novo* deletions, though inherited cases are reported.¹⁷ Attempts to develop a comprehensive phenotype profile are limited due to the deletion's low occurrence (~1 in 30,000 live births) and late-onset of some phenotypes, specifically the neuropsychiatric phenotypes.¹⁸ To date, all clinical cases and reports from the 3q29 registry corroborate that patients with this deletion display extensive variable phenotypic expressivity.^{17,19} This copy number variant confers a greater than 40-fold increased risk and has been identified as one of eight CNV risk loci for schizophrenia.^{15,16} The

3q29 deletion is also associated with increased risk for autism spectrum disorder, intellectual disability, and generalized anxiety disorder. ^{19–21} Aside from the neurodevelopmental phenotypes, 3q29 deletion patients also display physical abnormalities. Physical phenotypes include low birth weight, growth deficits, skull abnormalities (microcephaly, high nasal bridge, etc), and ocular abnormalities (microphthalmia, cataract, etc). Other reported phenotypes include heart defects, abnormal MRI, and gastroesophageal reflux disorder. ^{17,22} The Emory 3q29 Project clinical team is conducting comprehensive phenotyping on 3q29 deletion study subjects to better characterize the phenotype spectrum. ²³ The wide range of phenotypes, and observed variable phenotypic expressivity, suggests that deletion of the 3q29 interval affects many different molecular pathways.

The causal genetic element(s) of 3q29 deletion-associated phenotypes is not known. Of the 21 protein-coding genes, all but SLC51A (Slc1a) and ZDHHC19 (Zdhhc19) are expressed in either human or mouse brain. 24,25 The top candidate gene for the neurodevelopmental phenotypes in the interval are FBXO45, PAK2, and DLG1. 26 FBXO45 is of interest because of its expression at both the pre and post synaptic sites and identified role in synapse dynamics. FBXO45 encodes a ubiquitin ligase that regulates synaptic activity by degrading a synaptic vesicle priming factor. The absence of the priming factor prevents vesicle fusion and neurotransmitter release used for neuron communication. 27 PAK2 is another favored candidate gene because of its role in cytoskeletal dynamics at the synapse. 28 $Pak2^{+/-}$ mice display synaptic cytoskeleton deficits and autistic-like behavior. 29 DLG1 is the most popular candidate gene within the interval for the neurodevelopmental phenotypes given its role in synaptic plasticity via excitatory receptor trafficking in the brain. 30 A few studies identify an association between DLG1 and schizophrenia. Post mortem analysis of prefrontal cortex from schizophrenia patients display a

reduction in *DLG1* expression.³¹ A separate study examining exome sequences of schizophrenia patients shows an enrichment of variants in *DLG1* compared to controls.³² Mouse studies largely utilize conditional knockout models as *Dlg1* knockout mice die perinatally from respiratory failure. Mild, sex specific behavior deficits are observed in *Dlg1* brain specific conditional knockout mice.³³ Collectively these studies warrant further investigation of *DLG1* while also suggesting that *DLG1* is unlikely to be the only genetic driver for the observed phenotypes in 3q29 deletion patients. Work in *Drosophila* suggests a genetic interaction between *PAK2* and *DLG1*. Single gene heterozygous flies did not display a phenotype but *dlg/pak* transheterozygotes displayed reduced synapse number and circadian rhythm deficits.³⁴ These data suggest that complex phenotypes may be driven by more than one gene contained within the interval.

There has been limited focus on the other 16 genes expressed in brain within the 3q29 interval, but some of these genes share similar functions. Four genes (*TFRC*, *PCYT1A*, *SENP5*, *BDH1*) have been identified to function in metabolism and/or mitochondria function. Two genes (*TCTEX1D2*, *CEP19*) have identified functions in cilia formation and signaling. Another four genes (*UBXN7*, *RNF168 WDR53*, *FBXO45*) have been implicated in ubiquitination and ubiquitin-related modifications. New findings reported in a preprint article suggest that *NCPB2*, *DLG1*, *FBXO45*, *PIGZ*, and *BDH1* are functionally similar in their ability to disrupt cell cycle and apoptotic pathways. They also find that *NCBP2* acts as a modulator to enhance the deficits imposed by the other four genes individually.³⁵ A more in-depth summary of what is known about the remaining genes can be found in Table 1. Although informative, one should exercise caution in prioritizing candidate genes based on a review of the literature. Ideally there would be efforts to interrogate each gene's function in a systematic manner. In reality, the functional data

available for each gene is based on the specific interests of the experimenters. Incomplete functional profiles of genes within the 3q29 interval may initially deprioritize the genes as candidates, but it does not mean that they are not drivers of the 3q29 deletion phenotypes.

The remarkable increased risk for neurodevelopmental disorders associated with CNVs has prompted efforts to model these genomic alterations in mouse. These mouse models can help us better understand the etiology of the complex phenotypes. Until recently, efforts to study copy number variants in mice have been hindered by the inability to generate controlled genomic aberrations. The advent of Cre-loxP technology enabled the first targeted breakpoints using loxP sites.³⁶ Cre-mediated recombination occurs between two loxP sites and results in chromosome deletions, inversions, or even translocations depending on loxP site location and orientation. Though still used today, this chromosome engineering method has its limitations. The process in and of itself is incredibly labor-intensive. The targeting of loxP sites relies on the generation of insertion vectors which are then sequentially introduced into the mouse embryonic stem cell genome. Additional limitations exist in that the recombinase properties of Cre are less efficacious with increased distance between loxP sites. A selectable marker is used to detect cells with a recombination event after Cre transfection and further experiments are required to confirm the desired chromosome rearrangement. Although laborious, some of the first CNV mouse models were generated using the Cre-loxP chromosome engineering technique.^{37–39}

The recent discovery and development of CRISPR/Cas9 as a tool for chromosome engineering has made a complex, laborious process rather straight-forward and efficient.

CRISPR uses a guide RNA (gRNA) to target the Cas9 nuclease to the region of DNA where it will generate a double strand break. CNV deletions are generated by designing two gRNAs, one for each desired breakpoint. Double strand breaks in the DNA will activate repair via the non-

homologous end joining or homology directed repair pathway. Non-homologous end joining is the favored repair pathway and can result in nonspecific base pair insertions or deletions. ⁴⁰ The greatest advantage of this technique is the ability to bypass ES cell targeting by directly introducing the designed CRISPRs and Cas9 into a one-cell zygote. Genomic editing begins soon after introduction into the zygote and resulting offspring can be screened within one month. Additionally, Southern blot analysis or whole-genome sequencing can be used to confirm that only the desired genomic alteration occurred. One limitation of CRISPR/Cas9 technology is the possibility of off-target effects. ^{41,42} The resulting founder mice can be backcrossed multiple generations to recombine out the off-target mutations and minimize the likelihood of their effects. CRISPR/Cas9 technology has revolutionized the ability to generate targeted chromosome aberrations, including CNVs, by reducing the cost and time involved.

There is emerging evidence that suggests there are multiple genetic drivers for the complex phenotypes associated with CNVs, including the neurodevelopmental phenotypes. Mouse models of single genes within CNVs often do not recapitulate all of the phenotypes observed in models of the entire interval. For example, the learning and memory deficits observed 15q13.3 deletion mice are not observed in single candidate gene models. Similarly, models of candidate genes within the 16p11.2 interval do not display the abnormal brain morphology and motor coordination deficits observed in the 16p11.2 deletion mice. These data support that the interrogation of a single genes function and its effects when combined with the haploinsufficiency of neighboring genes is required to identify the driving genetic element(s) for each distinct phenotype.

Mouse studies of the 22q11.2 deletion have had limited success in identifying the causal genetic elements underlying observed complex phenotypes. In part, the challenges faced can be

attributed to the regions size and complexity. The 22q11.2 deletion is most often observed as the heterozygous deletion of a \sim 3 Mb interval with over 68 genes and 4 low copy repeats (LCRs). ⁴⁹ In stark contrast, the 3q29 deletion is a 1.6 Mb interval with only 21 genes and two LCRs. The syntenic interval on mouse chromosome 16 contains all 21 genes in the same order as human with an additional mouse specific gene (Bex6). The region is inverted to human with breakpoints synonymous to those identified in 3q29 patients. There are reported cases of asymptomatic individuals harboring an inversion of the 3q29 interval with breakpoints synonymous to those identified in those with the 3q29 deletion. ⁵⁰ These data suggest that the causative genetic element(s) of deletion phenotypes are contained within the interval rather than outside. The interval's relative low number of genes, low complexity, and synteny in mouse make it a great candidate for genetic dissection. To begin interrogating the interval for drivers of deletion-associated phenotypes, the Emory 3q29 Project mouse team made a mouse model using CRISPR/Cas9 to generate a heterozygous deletion of the 3q29 syntenic region in mouse (B6.Del16^{+/Bdh1-Tfrc}).

In this thesis I, in collaboration with the Emory 3q29 Project mouse team, set out to characterize the cognitive, behavioral, and physical deficits that exist in B6.Del16^{+/Bdh1-Tfrc} mice. In parallel, we interrogated the role of candidate gene *DLG1* in the B6.Del16^{+/Bdh1-Tfrc} phenotypes using B6.*Dlg1*^{+/-} mice. Many phenotypes observed in 3q29 deletion patients can be assessed in mice and serve as a starting place for our experiments. Specifically, we evaluated social interaction between stranger mice as a translational measure for the social deficits in autism spectrum disorder. The observed growth deficits in 3q29 patients prompted us to conduct a longitudinal study of growth in our mice. We will use the prominent phenotypes in our B6.Del16^{+/Bdh1-Tfrc} mice to define the critical region and potentially map the causal genetic

element(s). Given the evidence suggesting there are multiple, causal genetic elements for CNV phenotypes, instead of interrogating individuals genes I systematically subdivided the 3q29 interval. To narrow the critical region for phenotypes observed in B6.Del16^{+/Bdh1-Tfrc} mice, I generated two additional novel mouse models using CRISPR/Cas9 to subdivide the syntenic region into 11 genes apiece (B6.Del16^{+/Bdh1-Bex6} and B6.Del16^{+/Fbxo45-Tfrc}). The data in this thesis shows the utility of 3q29 deletion mouse models in narrowing the critical window and uncovering the underlying biology of complex, deletion-associated phenotypes.

Methods

Generation of mouse models using CRISPR/Cas9

To generate the full deletion in mouse, two guide RNAs were designed at the syntenic breakpoints in the mouse genome: gRNA 'A': TTCAGTGGTATGTAACCCCTGG at Chr.16:31,369,117 (GRCm38.p3) and gRNA 'B': CCTGAGCTGATTGGACAACTAG at Chr.16:32,634,414 (GRCm38.p3). An additional gRNA was designed between genes Bex6 and Fbxo45 in the mouse genome to generate the sub deletions in mouse: gRNA 'C': CCTTTAGTGGGTCTCCATTCAC at Chr.16:32,224,953 (GRCm38.p4). Single-cell C57BL/6N, 129, DBA and FVB zygotes were injected by the Emory Transgenic and Gene Targeting Core with 50 ng/μl of gRNA pairs (see Table 2) and 100ng/μl Cas9 RNA. Embryos were cultured overnight and transferred to pseudo pregnant females.

Dlg1^{+/-} mice on a 129/C57BL/6J mixed background were obtained from Dr. Jeffrey Miner (Washington University, St Louis, Missouri). The B6.Dlg1^{+/-} mice used were backcrossed to generation N6 with marker-assisted breeding (DartmouseTM, geiselmed.dartmouth.edu/dartmouse) to >99% congenicity on the C57BL/6N background. The DBA.Dlg1^{+/-} mice used were backcrossed to generation N4 to an average of 94% congenicity on the DBA background as no marker assisted breeding was used.

Screening for deletions using PCR and Southern Blot

Resulting pups were screened for the expected deletion via PCR using ear or tail genomic DNA. PCR primers were designed to detect the expected deletion and the wild-type (non-deleted) allele (Table 2).

PCR Conditions

PCR amplification was performed in a mixture of buffer, forward and reverse primers (0.5 μM), dNTPs, MgCl2 (~2 mM), Taq polymerase, and the DNA to be amplified (50 ng/rxn). Thermocycler settings for full deletion primers were as follows: 94°C for 5 min, 30 cycles at 94°C for 30 s, 56.7°C for 30 s, and 72°C for 60 s, then 1 cycle at 72°C for 5 min. Thermocycler settings for both sets of the sub deletion primers were as follows: 94°C for 5 min, 30 cycles at 94°C for 30 s, 57°C for 30 s, and 72°C for 60 s, then 1 cycle at 72°C for 5 min. Products were separated on a 2% agarose TBE gel.

Full deletion Southern blot

Full deletion pups were screened by Southern blot. Southern blots were adapted from a protocol as previously described. Briefly, 10 genomic DNA was digested overnight using the FastDigest XbaI from ThermoFisher Scientific (catalog number: FD0684). Fragments were separated on 0.8% agarose gel and transferred to a nylon membrane. The membrane was prehybridized with 14 mL hybridization buffer (350 mL 20% SDS, 75 mL 20x SSC, 100 g PEG8000, 250 mg heparin, water to 1L) and 500 uL salmon sperm at 65°C for 2-4 hours. A 542bp, p32 labeled DNA probe was generated using Invitrogen RadPrime DNA labeling system (Thermo Fisher Scientific, Waltham, MA) and the following primer pair: forward primer-ATTCAGGTCTTTAATGAGAACACAA and reverse primer-

TGAATAGTGGCTCTGTCTGAAG. The radiolabeled probe was added to 10 mL hybridization buffer with 500 uL salmon sperm and 20 uL cot1 DNA. The prehybridization solution was removed and the hybridization solution was added to the membrane and left overnight at 65°C. The following day the membrane was rinsed with 25 mL Buffer I (5 mL 20% SDS, 100 mL 20x SSC, water to 1 L) at room temperature. After rinsing, the membrane was washed for 15 minutes at 65°C with 50 mL of Buffer I followed by 30 minutes at 65°C with 50 mL of Buffer II (25 mL

20% SDS, 5 mL 20x SSC, water to 1 L). The membrane was laid on a phosphor screen overnight and imaged the following day.

Phenotyping of B6.Del16^{+/Bdh1-Tfrc} mice

All behavioral assays were conducted on 16 to 20-week-old mice. Behavioral assay sample size was 12-16 mice per sex per genotype. Behavior data collected was analyzed by unpaired t-test when comparing two groups. When comparing more than two groups, analysis was done by two-way, repeated measures ANOVA. Sidak's correction for multiple comparisons was used if a significant genotype effect or interaction was detected from the ANOVA. Mice were on a 12hr light/dark cycle with unrestricted food and water.

Growth curves

B6.Del $16^{+/Bdhl-Tfrc}$ [(female = 32 wild type, 34 mutant)(male = 33 wild type, 27 mutant)] and B6.Dlg $1^{+/-}$ [(female = 23 wild type, 25 mutant)(male = 36 wild type, 30 mutant)] mice were weighed weekly over 16 weeks, beginning at P8. Analysis was conducted in R using the package geepack by R. Pollak and M. Epstein. Generalized estimating equations were used to account for correlations observed in a single subject as a result of data being collected at multiple time points. Regression analysis was used for weight, genotype and age.

129.Del16^{+/Bdh1-Tfrc} [(female = 30 wild type, 32 mutant)(male = 52 wild type, 38 mutant)], FVB.Del16^{+/Bdh1-Tfrc} [(female = 21 wild type, 30 mutant)(male = 25 wild type, 18 mutant)], and DBA.*Dlg1*^{+/-} [(female = 4 wild type, 24 mutant)(male = 19 wild type, 24 mutant)] mice were weighed weekly, starting at P8, over 7 or 8 weeks depending on strain. Significance was determined using two-way, repeated measures ANOVA.

Social Interaction Behavior Paradigm

This paradigm was adapted from Yang et al.⁵² using a 58x46x38cm three-chamber apparatus constructed by The Emory Rodent Behavioral Core. Chambers were delineated as north, middle, and south with removable dividers between each chamber. The north and south chambers were 20cm long while the middle chamber was 18cm long. The subject mouse was placed in the middle chamber with the dividers in place for 8 minutes. The dividers were then removed, and the subject mouse was given 10 minutes to explore the entire, empty apparatus. After acclimation, the dividers were replaced with the mouse in the middle chamber. An empty cup and a cup with a stranger mouse were alternately placed in the north and south chambers. The dividers were removed, and the subject mouse was recorded for 10 minutes. Video footage was scored for duration of olfactory investigation with either the empty cup or cup with a stranger mouse.

Marble Burying Behavioral Assay

A 48x25x22cm plexiglass cage was filled with approximately 5 cm of evenly distributed corncob bedding. 20 black marbles were gently placed on top of the bedding in 5 rows of 4. The subject mouse was placed in the cage and given 30 minutes to bury the marbles. The mouse was removed after 30 minutes and a picture of the cage was taken for analysis. A marble was considered buried if >50% was covered by bedding. Three experimenters scored the photos while blinded to genotype. The average of the three scores for each subject mouse was reported.

Immunofluorescence

E15.5 pups were decapitated, and tail tissue was collected for genotyping. Heads were post-fixed in 4% PFA overnight. The heads were then dehydrated in 70% ethanol (EtOH) overnight, at minimum. The heads were placed in paraffin cassettes and submerged for 1 hour in each condition: 90% EtOH, 100% EtOH (repeat 3x), Xylene (repeat 2x). The cassettes were then

placed in liquid paraffin overnight and embedded the following day. Paraffin blocks were sectioned to 10 um thickness on a microtome and mounted on slides. Slides were deparaffinized and rehydrated before immunofluorescence.

For immunofluorescence, slides were blocked in 10% goat serum, 0.5% Tween-20 in 1X PBS for 1 hour. Primary antibody incubation was at 4°C overnight. Primary antibodies were Tbr1 (anti-rabbit, 1:500, Millipore #AB9616) and CleavedCaspase3 (anti-rabbit, 1:200, Cell Signaling #9661). Slides were then washed with 1X PBS and secondary antibody was applied and incubated at room temp for 1 hour. Signal was detected using fluorescent-conjugated Alexa 488 (Invitrogen A-11008) secondary antibody. Images were taken on a Leica DM6000 B microscope using QImaging Retiga EXi Fast1394 camera. Images were processed in ImageJ.

Results (My contributions are signified with "I/we")

CRISPR/Cas9 generated 3q29 full deletion mouse model

To mimic the 3q29 deletion in mouse, the Emory 3q29 mouse team designed two guide RNAs at these breakpoints, one proximal to *Bdh1* (CRISPR A) and one distal to *Tfrc* (CRISPR B) (Figure 1b). They used PCR to identify founder animals harboring the expected heterozygous deletion. Of the 23 animals born, 7 produced a PCR product indicating the expected heterozygous deletion. They confirmed the lack of gross rearrangements in full deletion animals by Southern blot. XbaI digested the genomic DNA and the radiolabeled probe hybridized to a 5.2 kb wild-type fragment and a 6.2 kb fragment on the deleted chromosome (Figure 1b).

PCR products for B6.Del16^{+/Bdh1-Tfrc} founders

The 3q29 mouse team sequenced the deletion PCR products of two B6.Del16^{+/Bdh1-Tfrc} founders used (#127 and #131) to determine the breakpoint location. The resulting sequences displayed different breakpoints by 21 bases which is likely a result of the non-homologous end joining repair pathway (see Table 3).⁵³

B6.Del16^{+/Bdh1-Tfrc} mice display growth deficits

Individuals with 3q29 deletion syndrome display reduced birth weight and difficulty gaining weight. To test for this phenotype in the B6.Del16^{+/Bdh1-Tfrc} mice, I collected weekly weights for 16 weeks beginning at P8 in collaboration with R. Pollak. Female B6.Del16^{+/Bdh1-Tfrc} mice weighed on average 2.24 grams less than their wild-type littermates (p<0.0001, Figure 2a). Male B6.Del16^{+/Bdh1-Tfrc} mice weighed on average 1.61 grams less than their wild-type littermates (p<0.0005, Figure 2b). Thus, we observed a growth deficit in both B6.Del16^{+/Bdh1-Tfrc} female and male mice when compared to their wild-type littermates. The observed growth deficits validate

using our novel rodent model to dissect the genetic drivers of deletion-associated, complex phenotypes.

We also weighed the B6. $DlgI^{+/-}$ mice and their wild-type littermates. The B6. $DlgI^{+/-}$ female mice weighed on average 0.78 grams less than their wild-type littermates (p<0.05, Figure 2c) and there was no significant difference between B6. $DlgI^{+/-}$ male mice and their wild-type littermates (Figure 2d). The observed growth deficits in B6. $DlgI^{+/-}$ female mice have smaller effect sizes than B6.Del16^{+/Bdh1-Tfrc} mice. These data indicate that DlgI may be contributing to the growth phenotype but is not the single causal gene.

Genetic background of Del16^{+/Bdh1-Tfrc} mice alters growth phenotype

Genetic background of subject mice can greatly influence the phenotypes.⁵⁴ To investigate this idea, the 3q29 mouse team generated the full deletion on three other mouse strains: DBA, 129, and FVB. They also backcrossed $Dlg1^{+/-}$ mice to be 94% congenic on the DBA background. I conducted growth curve analysis to investigate how genetic background may alter growth. These data are incomplete due to duration of collection (7-8 weeks) and small cohort size for some genotypes.

129.Del16^{+/Bdh1-Tfrc} mice displayed a growth phenotype in both sexes similar to B6.Del16^{+/Bdh1-Tfrc} mice. Female 129.Del16^{+/Bdh1-Tfrc} mice weighed on average 1.62 grams less than their wild type littermates (p<0.0001, Figure 3a) and male 129.Del16^{+/Bdh1-Tfrc} mice weighed 1.35 grams less than their wild type littermates (p<0.005, Figure 3b). We observed an alteration in the genotype-phenotype relationship in FVB.Del16^{+/Bdh1-Tfrc} mice. Female FVB.Del16^{+/Bdh1-Tfrc} mice weighed 0.95 grams less than their wild type littermates (p<0.05, Figure 3c). Notably, the reduced growth phenotype in B6.Del16^{+/Bdh1-Tfrc} female mice had a much larger effect size than

that of female FVB.Del16^{+/Bdh1-Tfrc} mice. Male FVB.Del16^{+/Bdh1-Tfrc} mice weighed slightly less than their wild type littermates, but the difference did not reach significance (p=0.07, Figure 3d).

I also weighed DBA. $Dlg^{+/-}$ mice. Preliminary results suggest that the genotype-phenotype relationship in DBA. $DlgI^{+/-}$ mice may be altered from the B6. $DlgI^{+/-}$ mice. Female DBA. $DlgI^{+/-}$ mice did not weigh significantly different from their wild type littermates, but the N for the wild types is not sufficient to draw conclusions (Figure 3e). Male DBA. $DlgI^{+/-}$ mice weighed 0.93 grams less compared to their wild type littermates (p=0.007, Figure 3f). My preliminary exploration of the growth phenotype in these other strains demonstrates that genetic background alters the genotype-phenotype relationship.

B6.Del16^{+/Bdh1-Tfrc} male mice have deficits in social interaction

We used the three-chamber social interaction paradigm to assess for social deficits. Difficulties in social communication is one of the hallmarks of autism spectrum disorder, which has been reported in 3q29 deletion patients.^{17,19} We placed the subject mouse in a three chamber apparatus with an empty cup and a cup with a stranger mouse in the north and south chambers. The subject mouse explored and interacted with the empty cup and/or cup with a stranger mouse for 10 minutes. I reviewed video footage of the paradigm and quantified duration of olfactory investigation with the stranger mouse in a cup or empty cup. I used olfactory investigation as a measure of social interaction. Wild-type mice spent significantly more time interacting with the stranger mouse compared to the empty cup (Figure 4a, female: $t_{26} = 7.176$, p<0.0001, male: $t_{28} = 4.018$, p<0.0005). Female B6.Del16^{+/Bdh1-Tfrc} mice displayed the same wild-type sociality ($t_{24} = 3.237$, p<0.005). Male B6.Del16^{+/Bdh1-Tfrc} mice did not demonstrate a preference for either the cup with the stranger mouse or the empty cup ($t_{28} = 1.769$, p = 0.0878). The lack of preference phenotype is translated into deficits in sociability.

In order to test whether heterozygosity of DlgI is the genetic driver of the observed deficits in B6.Del16^{+/Bdh1-Tfrc} male mice, we tested $DlgI^{+/-}$ mice for social interaction deficits (Figure 4b). $DlgI^{+/-}$ female and male mice did not display social deficits (female: $t_{24} = 4.716$, p<0.0001, male: $t_{24} = 2.846$, p<0.01), nor did their wild-type littermates (female: $t_{26} = 3.711$, p<0.005, male: $t_{22} = 6.29$, p<0.0001), thereby suggesting DlgI is not the singular contributor for the observed social deficits seen in B6.Del16^{+/Bdh1-Tfrc} male mice.

B6.Del16^{+/Bdh1-Tfrc} mice do not display anxiety-like behavior

We tested for anxiety-like behavior using the marble burying assay. In this assay we placed the subject mouse in a cage with 5 rows of 4 marbles placed on top of corn cob bedding. After 30 minutes the subject mouse was removed, and a photo of the cage was taken. Three experimenters, including myself, quantified the number of marbles buried in each photo and we reported an average of the three scores for each subject mouse (Figure 5). We observed no differences in the number of marbles buried between B6.Del16^{+/Bdh1-Tfrc} female and male mice compared to their wild-type littermates (Figure 5a, females: $t_{30} = 0.6147$, p>0.05, males: $t_{28} = 0.7167$, p>0.05). Similarly, we observed no differences between $Dlg1^{+/-}$ female and male mice relative to their wild-type littermates (Figure, 5b, females: $t_{25} = 0.22$, p>0.05, males: $t_{23} = 0.632$, p>0.05). These data indicate that the 3q29 deletion and Dlg1 do not contribute to a marble burying phenotype, but this does not rule out the contribution of these genetic elements in other anxiety-like behaviors.

B6.Del16^{+/Bdh1-Tfrc} mice display normal cortical plate development

Functional MRIs of schizophrenia patients display a reduction in cortical layer thickness. ⁵⁵ I examined the architectural integrity of B6.Del16^{+/Bdh1-Tfrc} brains at the peak of neurogenesis (E15). To examine cortical layer development, I used an antibody against T-box,

Brain 1 (*Tbr1*) in E15.5 embryos. Tbr1 is a T-box gene that codes for a transcription factor involved in regulating cortical development.⁵⁶ I saw no gross differences in layer thickness relative to wild-type littermates (Figure 6). I also assessed for excessive cellular death in these slices using an antibody against CleavedCaspase3. I saw no obvious evidence of excessive cellular death in B6.Del16^{+/Bdh1-Tfrc} brains compared to wild-type controls (not quantified, Figure 6). Together these data suggest that the 3q29 deletion does not alter apoptosis or cortical layer establishment in E15.5 embryos.

CRISPR/Cas9 generation of 3q29 sub deletion mouse models

The B6.Del16^{+/Bdh1-Tfrc} mice recapitulated some of the distinct, complex phenotypes observed in 3q29 deletion patients. To narrow the critical region for each distinct phenotype, I systematically subdivided the 3q29 interval and observed the effects on established, full deletion phenotypes. I designed a third guide RNA between *Bex6* and *Fbxo45* (CRISPR C) to subdivide the interval into two regions containing 11 genes apiece (Figure 1c). Mice were injected with CRISPR A, from the full deletion, and CRISPR C to generate the proximal sub deletion from *Bdh1* to *Bex6* (B6.Del16^{+/Bdh1-Bex6}). I used PCR to identify founder animals harboring the expected heterozygous sub deletion. Of the 8 animals born from the proximal sub deletion injections, 3 animals had a PCR product indicative of the expected deletion. Separate injections of CRISPR B, from the full deletion, and CRISPR C generated mice harboring the adjacent, distal sub deletion from *Fbxo45* to *Tfrc* (B6.Del16^{+/Fbxo45-Tfrc}). Of the 39 animals born from the distal sub deletion injections, 4 had a PCR product indicating the presence of the expected heterozygous deletion.

PCR products for B6.Del16^{+/Fbxo45-Tfrc} founders

I sequenced the deletion PCR products for all animals with the expected distal sub deletion to determine the breakpoint location. I did not identify any two potential founders carrying identical breakpoints indicating chew back at the Cas9 cut site during repair via non-homologous end joining. I used founders 52 and 79 to backcross to generation N4 and obtain cohorts for analysis because their breakpoints were only 2 base pairs different (see Table 3). These animals are following the same breeding scheme as the full deletion animals and cohorts will be bred for analysis at generation N4.

Discussion

The Emory 3q29 mouse team generated a novel mouse model harboring the 3q29 deletion as part of a collective effort to better understand the genetic drivers of complex, deletion-associated phenotypes. We conducted a broad range of analyses to establish a phenotypic profile and discern the biological consequences of the 3q29 deletion. First, we found that B6.Del16^{+/Bdh1-Tfrc} mice displayed persistent growth deficits reminiscent of those observed in individuals with 3q29 deletion (Figure 2a-b). These findings were recently replicated in another 3q29 mouse model generated with Cre-loxP technology.⁵⁷ Growth is a complex phenotype influenced by both genetic and environmental factors. The effects of these factors converge on a single biological process: the cell cycle.⁵⁸ Given this, candidate genes in the 3q29 interval for the observable growth deficits could be those implicated in the cell cycle (NCBP2, DLG1, FBXO45, PIGZ, BDH1). Additional analyses link growth arrest with repression of genes involved in metabolism and mitochondria function.⁵⁹ These data suggest additional candidate genes for the growth deficits are those with roles in metabolism and mitochondria function (PCYT1A, BDH1, SENP5, TFRC). We analyzed $Dlg1^{+/-}$ mice to determine whether Dlg1 was the causal genetic element for observed growth deficits. Only female $Dlg l^{+/-}$ mice displayed a significant growth deficit compared to their wild type littermates (Figure 2c). The effect size observed was much smaller than those observed in the B6.Del16^{+/Bdh1-Tfrc} mice suggesting that *Dlg1* may be contributing to the growth phenotype in female mice, but is not the only contributing genetic element.

As previously stated, phenotypes manifest variably in mice of different genetic backgrounds. ⁵⁴ We generated and assessed growth in two additional mouse models of the 3q29 deletion, on the FVB and 129 genetic background, to thoroughly define the relationship between

the 3q29 deletion genotype and growth phenotype. As predicted, I observed changes in the genotype-phenotype relationship depending on the mouse genetic background. FVB.Del16^{+/Bdh1-Tfrc} male mice did not weigh significantly less than their wild type littermates (Figure 3d). FVB.Del16^{+/Bdh1-Tfrc} females weighed less than their wild type littermates with a much smaller effect size compared to B6.Del16^{+/Bdh1-Tfrc} female mice (Figure 3c). The 129.Del16^{+/Bdh1-Tfrc} mice displayed growth deficits similar to those observed in the B6.Del16^{+/Bdh1-Tfrc} mice (Figure 3a and 3b). The reported alterations in the genotype-phenotype relationship suggest there are genetic modifiers acting in some mouse strains, and not others, to exacerbate or diminish the growth phenotype.

The strong association of the 3q29 deletion with neurodevelopmental disorders prompted us to evaluate cognitive and behavioral function in the B6.Del16^{+/Bdh1-Tfrc} mice. Twenty-five to 30% of individuals with the 3q29 deletion report diagnosis of autism spectrum disorder.^{17,19,22} This neurodevelopmental disorder has a 4:1 male bias and is characterized by deficient social skills, language difficulties, and restrictive behaviors.⁶⁰ We assessed for deficits in social interaction via the three-chamber test in B6.Del16^{+/Bdh1-Tfrc} mice as an endophenotype for autistic behaviors. B6.Del16^{+/Bdh1-Tfrc} male mice display social interaction deficits but B6.Del16^{+/Bdh1-Tfrc} female mice do not (Figure 4a). Studies on the Cre-loxP 3q29 mouse model also found deficits in social behavior using the reciprocal social interaction test.⁵⁷ We tested the $Dlg1^{+/-}$ mice in the three-chamber paradigm and did not find any deficits eliminating Dlg1 as the single driver for the social deficits observed in B6.Del16^{+/Bdh1-Tfrc} male mice (Figure 4b). The identified sexspecific social deficits in B6.Del16^{+/Bdh1-Tfrc} mice align with the sex differences observed in autism and suggest that there may be sex-specific molecular mechanisms underlying these

phenotypes. Future studies should include investigation of complex phenotypes in a sex-specific manner with the possibility of unveiling novel differences.

Anxiety is another prominent neuropsychiatric phenotype in 3q29 deletion patients. 19 We assessed anxiety with the marble burying assay and did not observe increased anxiety in male or female B6.Del16^{+/Bdh1-Tfrc} mice (Figure 5a). These findings are in stark contrast to the 3q29 deletion human data. One explanation for the disparity is that there are multiple tests for evaluating anxiety-like behaviors in mice, including marble burying, open-field, and elevated plus maze. Anxiety is a complex phenotype with many different features and each task is designed to assess a subset of those features.⁶¹ The variable expressivity of anxiety in individuals with the 3q29 deletion may explain why some tasks reveal phenotypes and others do not. Another plausible explanation for the absence of anxiety-like behavior is the presence of modifier alleles in the C57BL/6 mouse strain that mask the phenotype. We can begin testing this hypothesis by putting the FVB.Del16^{+/Bdh1-Tfrc} and 129.Del16^{+/Bdh1-Tfrc} mice through the marble burying assay. It is understood that this would not be a comprehensive analysis given there are many more mouse strains than the two listed. The absence of a marble burying phenotype in B6.Del16^{+/Bdh1-Tfrc} mice does not rule out the genetic contribution of the 3q29 deletion to other anxiety-like behaviors.

I began exploring the hypothesis that the underlying molecular mechanism for the reduced growth phenotype is dysregulation of the cell cycle by staining embryonic brain slices for a marker of apoptosis, cleaved caspase-3. I decided to evaluate cellular death at embryonic day 15.5 when neurogenesis in the brain is at its peak.⁶² There were no observable differences in apoptosis between E15.5 wild type and B6.Del16^{+/Bdh1-Tfrc} embryos (Figure 6). During neurogenesis in the cerebral cortex, cells replicate, divide, and migrate to establish an organized

layer establishment, *Tbr1*, in E15.5 embryos to assess for dysfunction in these cellular processes. ⁵⁶ The altered thickness of the cortical layers observed in individuals with schizophrenia suggests a functional relevance of alterations in neurogenesis and, specifically, cortical layer establishment. I saw no gross differences in layer thickness in B6.Del16^{+/Bdh1-Tfrc} embryos compared to wild type (Figure 6). Interestingly, recent findings show a remarked decrease in number of parvalbumin expressing inhibitory neurons in the cortex. ⁵⁷ I did not detect these difference in my staining because *Tbr1* is highly expressed in excitatory, rather than inhibitory, neurons. ⁵⁶ Additional studies are required to support or refute the proposed hypothesis that dysregulation of the cell cycle underlies the growth phenotype. Obvious next steps would be to stain for cleaved caspase-3 at different time points and include a proliferative marker.

The pronounced growth and social phenotypes in B6.Del16^{+/Bdh1-Tfrc} mice will be used as a tool to determine if our systematic sub deletion strategy is a tractable way to identify the genetic drivers of these phenotypes. In order to find the critical genetic element(s) in the 3q29 interval responsible for the observed phenotypes, we will sub divide the interval in an unbiased, step-wise fashion in mouse and assess the phenotypes. I generated the first two sub deletion mouse models, each with heterozygous deletions of either the proximal (B6.Del16^{+/Bdh1-Bex6}) or distal (B6.Del16^{+/Fbxo45-Tfrc}) 11 genes. The B6.Del16^{+/Bdh1-Bex6} founders initially had breeding difficulties and injections were repeated. The breeding scheme underway for the B6.Del16^{+/Bdh1-Bex6} and B6.Del16^{+/Fbxo45-Tfrc} mice is the same as the full deletion mice and cohorts for analysis will be generation N4.

The data in this thesis has laid the foundation for future experiments and the genetic dissection of the 3q29 interval. Some of the outstanding questions can be addressed with a

combination of the mouse models we generated and efforts by the International Mouse Phenotyping Consortium (IMPC) to prioritize, generate and phenotype single gene loss of function alleles in C57BL/6 mice for the 21 genes in the 3q29 interval. Below, I will lay out how these tools can be leveraged to address some of the outstanding questions.

Are the genetic drivers of the social and growth phenotypes within the 3q29 interval?

The presence of the growth and social phenotypes in sub deletion mice would confirm that the genetic drivers are within the 3q29 interval. There are three different ways in which the growth and social phenotypes can manifest in the B6.Del16^{+/Bdh1-Bex6} and B6.Del16^{+/Fbxo45-Tfrc}. 1) The growth and social phenotypes can segregate together with one sub deletion or the other thereby narrowing the critical window to 11 genes. Next steps would include subdividing the region again and assess how the phenotypes segregate to narrow the critical window even further. 2) The growth and social phenotypes segregate with different sub deletions. This result will suggest that the two complex phenotypes are being driven by different genetic elements within the 3q29 interval. Next steps would be the same as if the phenotypes segregated together.

3) A more complex result would be the manifestation of diminished growth and social phenotypes in both sub deletions. This result will suggest additive effects of multiple genes across the 3q29 interval. The complexity arises in the fact that it cannot be discerned whether the phenotypes are a result of the additive effects of a few or all of the genes.

Conversely, if the growth and social phenotypes are not observed in sub deletion mice, there are two possible reasons. The manifestation of these phenotypes could require the synergistic interaction between multiple haploinsufficient genes. Alternatively, a gene within the interval is a regulator for the causal genetic element(s) located outside of the interval. These possibilities can be tested by breeding B6.Del16^{+/Bdh1-Bex6} and B6.Del16^{+/Fbxo45-Tfrc} mice to

produce a new mouse model harboring the proximal and distal sub deletion in trans (B6.Del16^{Bdh1-Bex6/Fbxo45-Tfrc}). If neither sub deletion alone display the phenotypes by the B6.Del16^{Bdh1-Bex6/Fbxo45-Tfrc} mice do, it supports the hypothesis that synergistic interactions between genes across both sub deletions are necessary for the presentation. If B6.Del16^{Bdh1-Bex6/Fbxo45-Tfrc} mice do not exhibit the phenotypes, it supports the hypothesis that regulatory genes are acting on the drivers outside of the interval. Another less explored explanation is that the observed phenotypes manifest from disruptions in chromatin structure within the interval.⁶³ Is Dlg1 a modifier of 3q29 deletion-associated phenotypes?

Variable expressivity of 3q29 deletion-associated phenotypes in humans suggest the presence of genetic modifiers. A genetic modifier is defined as an element that alters the phenotypic expression of another gene or genes.⁶⁴ The diminished growth deficits observed in B6.*Dlg1*^{+/-} mice implicate *Dlg1* as a potential modifier for the growth phenotype. If the growth deficits were to segregate in the distal sub deletion, future studies could test the modifier function of *Dlg1* by crossing B6.*Dlg1*^{+/-} mice with the B6.Del16^{+/Fbxo45-Tfrc} mice to generate mice harboring both the sub deletion and haploinsufficiency of *Dlg1*. Exacerbation or reduction of the growth deficits in these mice would support the hypothesis that *Dlg1* is a genetic modifier for the growth deficits observed in the 3q29 deletion.

How can key genetic elements be identified using the sub deletion strategy?

Our step-wise sub deletion strategy is an unbiased approach that has the potential to identify functionally relevant genetic elements underlying complex 3q29 deletion-associated phenotypes. Genes identified by IMPC as having large effects on distinct phenotypes would warrant generation of mouse models harboring various combinations of the sub deletions and single gene mutations. Examination of these models for exacerbated or diminished phenotypes

would begin dissecting the interactions between each gene and other elements within the interval This approach could identify which combination of genetic elements in the interval is driving each phenotype.

The sub deletion strategy is also capable of uncovering whether distinct, complex phenotypes are driven by the same, different, or overlapping genes. The identification of overlapping drivers for behavioral deficits observed in B6.Del16^{+/Bdh1-Tfrc} mice would warrant future studies interrogating the molecular pathways associated with that gene. The 3q29 mouse models we generated will continue to be remarkably useful in the genetic dissection of the 3q29 interval and identification of genetic drivers underlying its complex phenotypes, like neuropsychiatric disorders.

| | Summary | Mouse model data |
|-----------|---|---|
| NRROS | Expressed in immune cells of the central | Nrros-/- mice display severe motor deficits |
| | nervous system. Regulates reactive | and die before 6 months. ⁶⁶ |
| | oxygen species. Required for microglia | |
| | differentiation and development. ⁶⁵ | |
| PCYT1A^ | Encodes rate-limiting enzyme for | Pcytla ^{-/-} mice are embryonic lethal E3.5 |
| | synthesis of cell membrane lipid | Pct1a ^{+/-} mice show 50% enzyme activity |
| DDIIIA | phosphatidylcholine (PPC). ⁶⁷ | does not affect PPC synthesis in adults. ⁶⁷ |
| BDH1^* | Encodes mitochondrial membrane | Cardiac-specific <i>Bdh1</i> ^{-/-} mice display |
| | enzyme that helps synthesize beta- | worsened heart failure upon exposure to |
| | hydroxybutyrate, a metabolic intermediate | stressors compared to their wild type |
| | that is a key regulator in metabolic | littermates. ⁶⁹ |
| SENP5^* | disease pathogenesis. 68 | Carre 5-/- mais a sura in distinguish abla from |
| SENP3' | Encodes an enzyme active in the nucleus and mitochondria. Reduction of this | Senp5 ^{-/-} mice are indistinguishable from wild type littermates. ⁷³ |
| | enzyme results in altered mitochondrial | who type intermates. |
| | function and morphology. 70,71 Also | |
| | required for cell division. ⁷² | |
| TFRC^ | Encodes a transferrin receptor that is | <i>Tfrc</i> -/- mice are embryonic lethal E12.5 |
| | important for iron uptake. | from anemia and hypoxia. <i>Tfrc</i> ^{+/-} mice are |
| | Receptor functions in regulating | indistinguishable from wild type by |
| | mitochondrial fusion and function. ⁷⁴ | display deficits in iron homeostasis. ⁷⁵ |
| MFI2 | Encodes a melanotransferrin proteins with | <i>Mfi2</i> mice are indistinguishable from wild |
| | similar sequence and structure to TFRC. | type littermates, no deficits in iron uptake |
| | Suggested role in tumorigenesis and | or metabolism. ⁷⁷ |
| | proliferation. ⁷⁶ | |
| RNF168' | Encodes a ubiquitin ligase that play a | <i>Rnf168</i> ^{-/-} mice are indistinguishable from |
| | critical role in double strand break | wild type but display age-dependent |
| | repair. ⁷⁸ | reduced male fertility. ⁷⁹ |
| UBXN7' | Regulates ubiquitin ligase activity by | Ubxn7 ^{-/-} mice are preweaning lethal. E18.5 |
| | binding ubiquitinated proteins. ⁸⁰ | embryos show growth and skull deficits. ⁷³ |
| WDR53' | Adaptor protein for interactions between | |
| | ubiquitin ligase and target proteins. ⁸¹ | T 1 10-/- 1 1 1 72 |
| TCTEX1D2• | Protein involved in trafficking to, and | Tctex1d2 ^{-/-} male mice are infertile. ⁷³ |
| CED 100 | possibly within the cilium. | C10 |
| CEP19• | Homozygous mutations found in | Cep19 ^{-/-} mice are obese, glucose intolerant, |
| | ciliopathy patients. 82 Protein localizes to | insulin resistant, and infertile due to |
| | the mother centriole and is involved in | degradation of the sperm tail. ⁸⁴ |
| NCBP2* | cilia assembly. ⁸³ Modulator that enhances the cell cycle or | <i>Ncbp2</i> ^{-/-} mice are preweaning lethal. |
| IVCDI 2 | apoptotic pathway deficits imposed by | Ncop2 indee are preweating tetrial. $Ncbp2^{+/-}$ male mice display an increased |
| | DLG1, FBXO45, PIGZ, & BDH1 | anxiety-related response. ⁷³ |
| | individually. ³⁵ | annicry-related response. |
| | marviduany. | |

Table 1. Summary of functional data for brain-expressed genes in the 3q29 interval. *SLC51A* and *ZDHHC19* are not expressed in brain. ^ genes function linked to metabolic pathways and/or mitochondrial function. ' genes function in ubiquitination or ubiquitin-related modifications. • genes function in cilia and/or associated with ciliopathies. * genes function in the cell cycle and apoptotic pathways.

| CACCAATAGTGAGGCGGTTT Product size: ~330 bp | gRNA B: CCTGAGCTGAT TGGACAACTAG | |
|--|---|--|
| Proximal Forward: ATGCATGTTCATGCTGTGGT Distal Reverse: | gRNA C: CCTTTAGTGGG TCTCCATTCAC | Distal sub deletion B6.Del16 ^{+/Fbxo45-Tfrc} |
| GTTACTCCCTTTTGCCTCCC Product size: | gRNA C: CCTTTAGTGGG TCTCCATTCAC | |
| Proximal Forward: CCCTCCTTCCTCAATCACTG Distal Reverse: | gRNA A: TTCAGTGGTAT GTAACCCCTGG | Proximal sub deletion B6.Del16 ^{+/Bdh1-Bex6} |
| Product size: ~400 bp | CCTGAGCTGAT TGGACAACTAG | |
| Distal Reverse: TGCCACTCTTCAGCTCATTG | GTAACCCCTGG gRNA B: | |
| Proximal Forward: CCCTCCTTCCTCAATCACTG | gRNA A: TTCAGTGGTAT | Full deletion B6.Del16 ^{+/Bdh1-Tfrc} |
| Deletion PCR primers | gRNA pairs | |
| T C Q Q Q | Deletion PCR primers Proximal Forward: CCCTCCTTCCTCAATCACT Distal Reverse: TGCCACTCTTCAGCTCATT Product size: ~400 bp Proximal Forward: CCCTCCTTCCTCAATCACT Distal Reverse: GTTACTCCCTTTTTGCCTCCC Product size: Proximal Forward: ATGCATGTTCATGCTGTGC | irs GGTAT CCTGAT ACTAG CTGGTAT CCTGG GTGGG GTGGG GTGGG |

 $Table\ 2.\ Primer\ and\ guide\ RNA\ sequences\ for\ 3q29\ mouse\ models.$

| B6.Del16 ^{+/Fbxo45-Tfrc} Founder # 79 CAAG CCTCC ACGTC | B6.Del16 ^{+/Fbxo45-Tfrc} Founder # 52 TCCC7 GTGA | B6.Del16+/Bdh1-Tfic AGGC Founder # 131 GAAG TTTTA TATGA ACCGG CTGGG | B6.Del16 ^{+/Bdh1-Tfrc} Founder # 127 GTAT0 GGCA TCCT0 AGGCA AGGA | Breakp |
|---|--|---|--|---------------------|
| ATTGTATGGATTCTGGGGAATAAACTCAAAATCCTCAGGCTCAATGCCAAGAGCTCTTACCCCCGAGCCATCTCTGCCCCTACCAGCAG TTCCCTCCCTCCCTCCTGTCTGTCTTCTGTTCCTCTTTTATGTAGCAAACTCTCTGTGACTCAGTGGCACGCCTCTCTTTTATGTAGCAAACTCTGTGACTCAGTGGCACGCCTCTCTTTGCA | ATTGTATGGATTCTGGGGAATAAACTCAAATCCTCAGGCTCAATGCCAAGAGCTCTTACCCCCGAGCCATCTCTGCCCCCTACCAGCAG CCCCCAAGAGCCTCTCTCTCTCTCTCTCTCTTTTATGTAGCAAACCTCAACTCTCAGTGGCACGCCTCTCTTTGCA | AGGCATTTTCTCAAGTAAGGTTCCCTCTTTTCTGATGACTCTACCTT GTATCAAGTTGACATAAAGCTGCCAAGATCTGTCACCAGCTTCAGT GAAGACAGAGTTCCCTCCCTCCCTCCTGTCTGTCTCTCTC | AGGCATTTTCTCAAGTAAGGTTCCCTCTTTTCTGATGACTCTACCTT GTATCAAGTTGACATAAAGCTGCCAAGATCTGTCACCAGCTTCAGT GGTATGAAGTTGACATAAAGCTGCCAAGATCTGTCACCAGCTTCAGT GGTATGTAGGAGACAGACAGAGAGAGAGAGTTCCCTCTCCC TCCTGTCTGTCTTCTGTTCCTCTTTTATGAGAAACGTGACTCAGT GGCACGCCTCTCTTGCACTCCTATGAGATATCACTGAAATTATTAT TATTATTATAAAAAAAGAGAAACCGCCTCACTATTGGTGCCAAGAA AGGATTTTTGGTGTCTAAGCATCTGGCCTCTCTGGGAACCAATGAG AGGATTTTTTTGGTGTCTAAGCATCTGGCCTCTCTGGGAACCAATGAG | Breakpoint Sequence |

Table 3. Breakpoint PCR sequences for founder animals. Bold letters signify breakpoint differences.

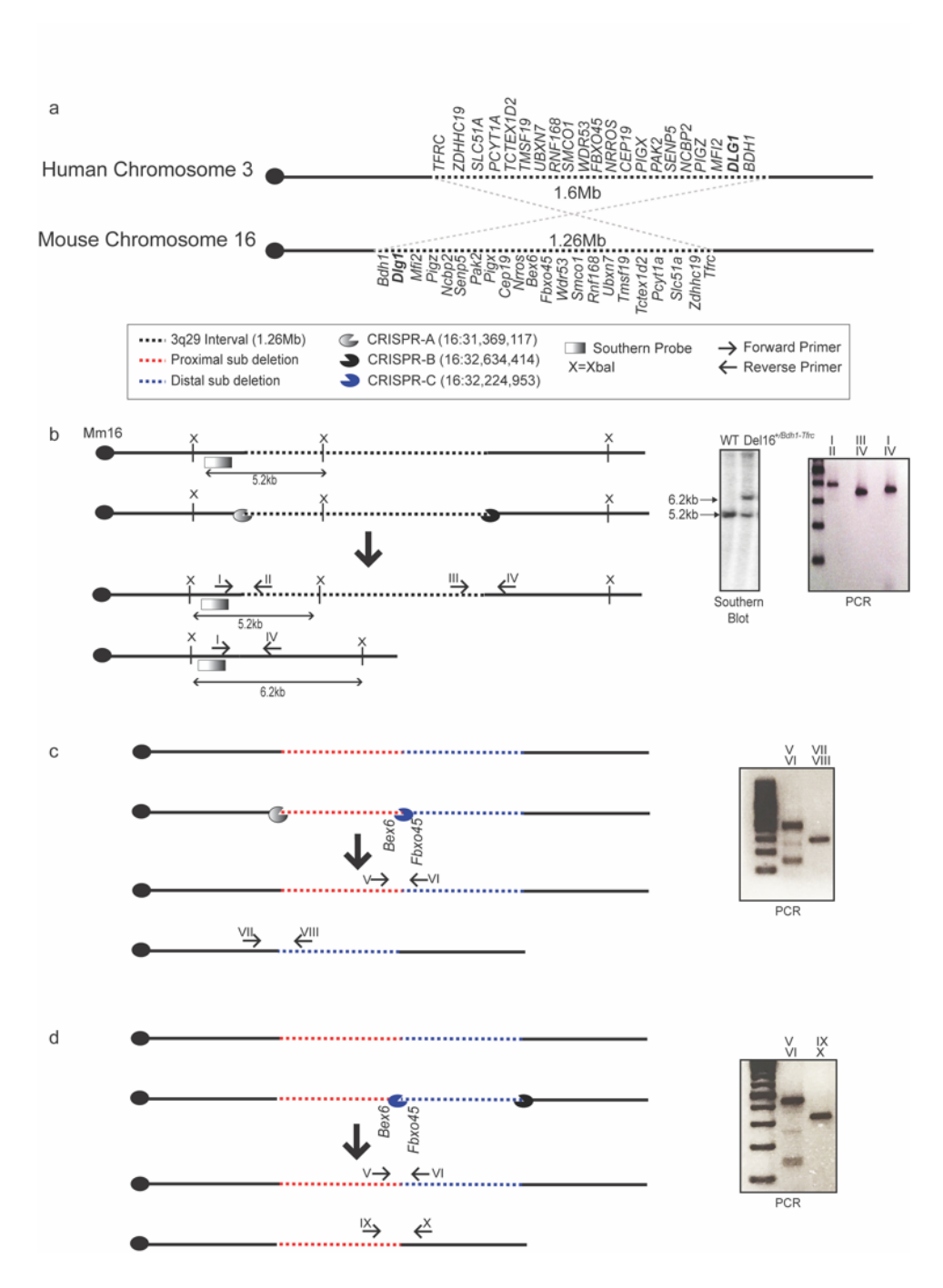


Figure 1. CRISPR/Cas9 generation of 3q29 deletion mouse models.

a) The 3q29 interval is on chromosome 3 in human and inverted on chromosome 16 in mouse. b) CRISPR A (chr16:31,369,117) and CRISPR B (chr16:32,634,414) were designed to mimic the reported human breakpoints and used to generate a heterozygous deletion of the 3q29 region. PCR and southern blot were used to confirm deletion presence. c) CRISPR C (chr16:32,224,953) was designed to generate sub deletions of the 3q29 interval. The proximal, heterozygous sub deletion was generated using CRISPR A and CRISPR C and confirmed with PCR. d) CRISPR C and CRISPR B were used to generate the distal, heterozygous sub deletion. PCR was used to detect the expected sub deletion.

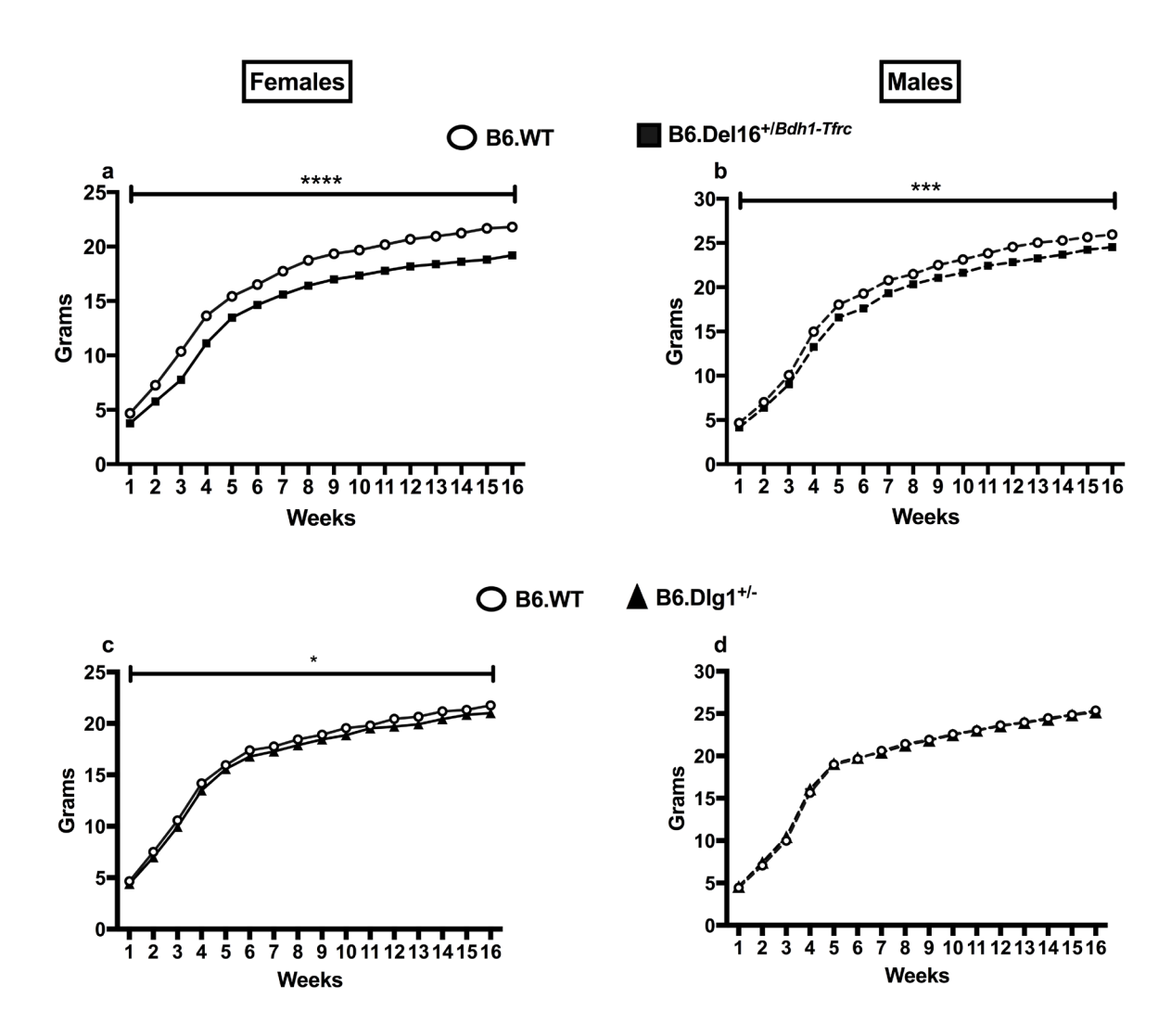


Figure 2. B6.Del $16^{+/Bdh1-Tfrc}$ female and male mice display robust growth deficits while B6. $Dlg1^{+/-}$ females display subtle growth deficits.

a) B6.Del16^{+/Bdh1-Tfrc} female mice weigh less than their wild type littermates (N = 34 wild type, 32 mutant) b) B6.Del16^{+/Bdh1-Tfrc} male mice weigh less than their wild type littermates (N = 33 wild type, 27 mutant) c) B6.Dlg1^{+/-} female mice weight less than their wild type littermates (N = 23 wild type, 25 mutant) d) B6.Dlg1^{+/-} male mice weigh the same as their wild type littermates (N = 36 wild type, 30 mutant). *p<0.05, ***p<0.0005, ****p<0.0001.

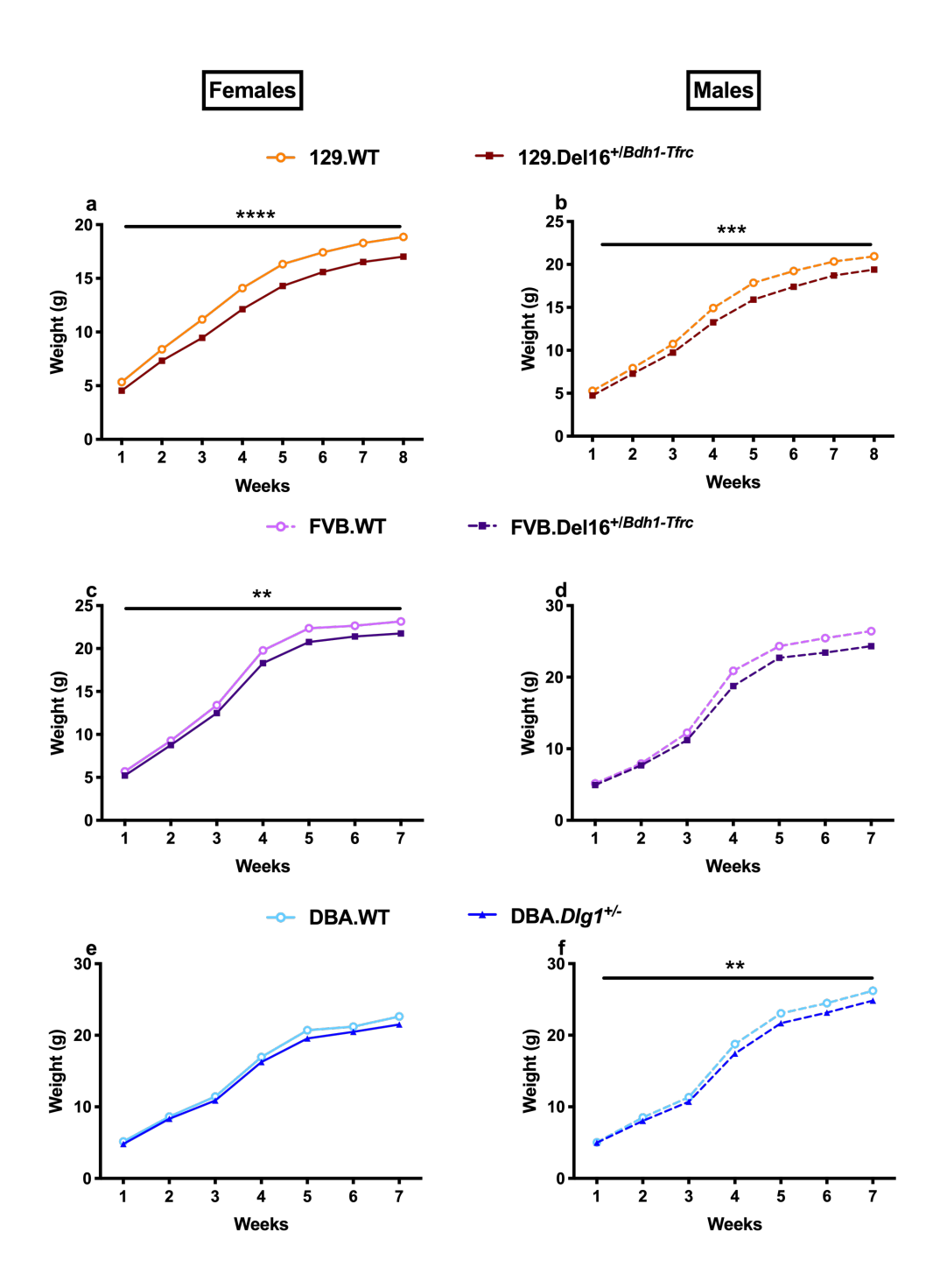


Figure 3. Mouse genetic background alters the growth deficit phenotype. a) $129.\text{Del}16^{+/Bdhl-Tfrc}$ female mice weigh less than their wild type littermates (N = 30 wild type, 32 mutant). b) $129.\text{Del}16^{+/Bdhl-Tfrc}$ male mice weigh less than their wild type littermates (N = 52 wild type, 38 mutant). c) FVB.Del $16^{+/Bdhl-Tfrc}$ female mice weigh slightly less than their wild type littermates (N = 21 wild type, 30 mutant). d) FVB.Del $16^{+/Bdhl-Tfrc}$ male mice weigh the same as their wild type littermates (N = 25 wild type, 18 mutant) e) DBA. $Dlg1^{+/-}$ female mice weigh the same as their wild type littermates (N = 4 wild type, 24 mutant) f) DBA. $Dlg1^{+/-}$ male mice weigh slightly less than their wild type littermates (N = 19 wild type, 24 mutant). Significance was determined by two-way ANOVA. **p<0.05, ***p<0.005, ****p<0.0001

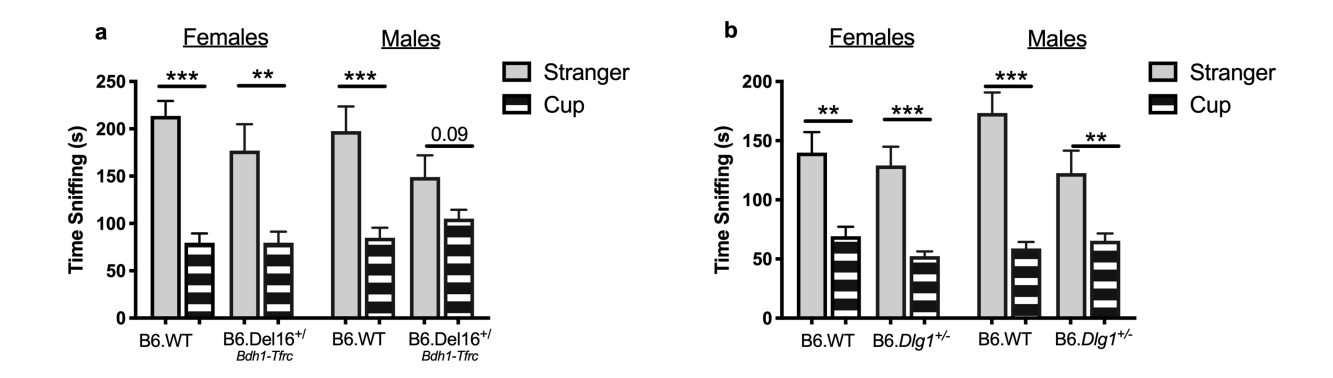


Figure 4. B6.Del16^{+/Bdh1-Tfrc} male mice display social impairment.

a) B6.Del16^{+/Bdh1-Tfrc} female mice and their wild type littermates spent more time interacting with the stranger mouse in a cup versus the empty cup (N = 14 wild type, 14 mutant). B6.Del16^{+/Bdh1-Tfrc} male mice displayed no preference between the stranger mouse in a cup and the empty cup (p = 0.09) while their wild type littermates preferred to interact with the stranger mouse in a cup (N = 15 wild type ,15 mutant). b) B6.Dlg1^{+/-} female mice and their wild type littermates spent more time interacting with the stranger mouse in a cup compared to the empty cup (N = 14 wild type, 13 mutant). B6.Dlg1^{+/-} male mice and their wild type littermates spent more time interacting with the stranger mouse in a cup compared to the empty cup (N = 12 wild type, 13 mutant). ***p<0.0005, **p<0.01.

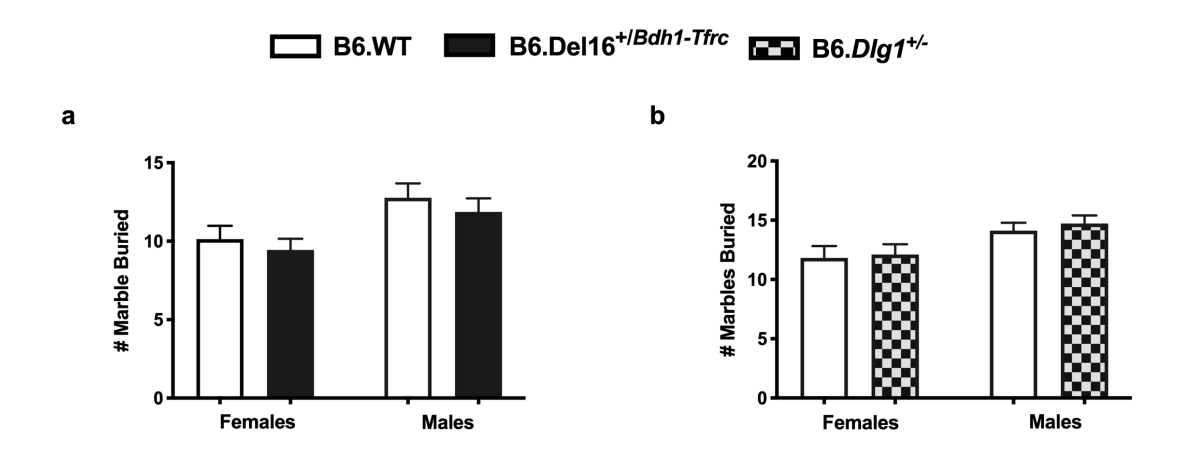


Figure 5. B6.Del16^{+/Bdh1-Tfrc} and B6.Dlg1^{+/-} do not display altered anxiety.
a) B6.Del16^{+/Bdh1-Tfrc} female and male mice bury the same number of marbles compared to their wild type littermates [N = (female: 16 wild type, 16 mutant), (male: 15 wild type, 15 mutant)]. b) B6.Dlg1^{+/-} female and male mice bury the same number of marbles compared to their wild type littermates [N = [(female: 14 wild type, 13 mutant), (male: 12 wild type, 13 mutant)].

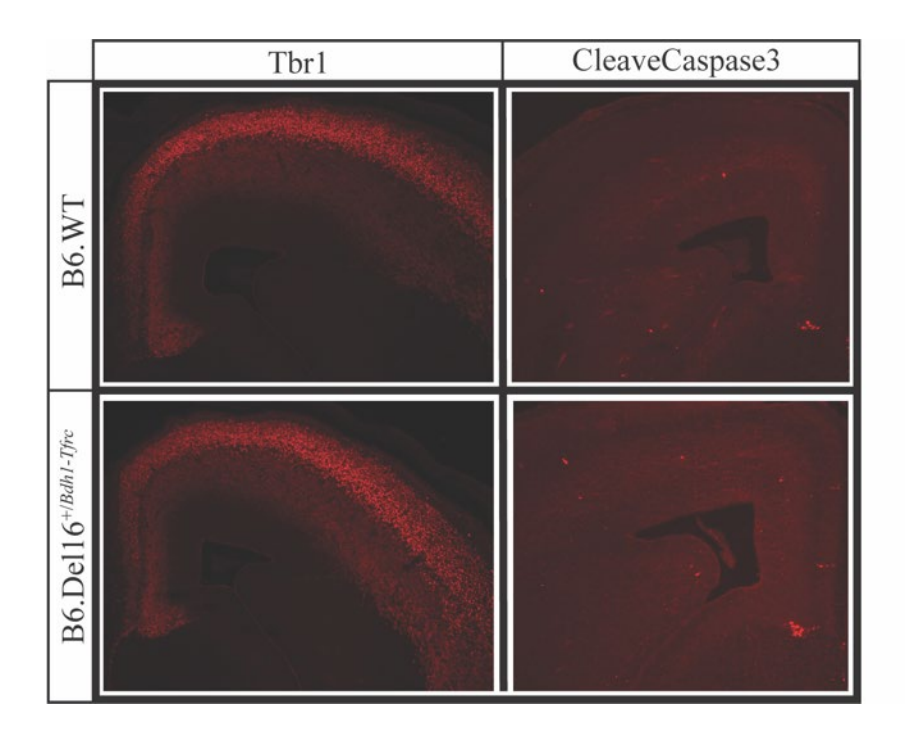


Figure 6. B6.Del16^{+/Bdh1-Tfrc} embryos have normal cortical plate development and cell death. E15.5 B6.Del16^{+/Bdh1-Tfrc} embryos display similar Tbr1 and CC3 staining compared to their wild type littermates (N = 3 wild type, 3 mutant).

References

- 1 McGuffin P, Tandon K, Corsico A. Linkage and association studies of schizophrenia. *Curr Psychiatry Rep* 2003;**5**:121–7. https://doi.org/10.1007/s11920-003-0028-y.
- 2 Rietveld MJH, Hudziak JJ, Bartels M, van Beijsterveldt CEM, Boomsma DI. Heritability of attention problems in children: I. cross-sectional results from a study of twins, age 3-12 years. *Am J Med Genet Part B Neuropsychiatr Genet Off Publ Int Soc Psychiatr Genet* 2003;**117B**:102–13. https://doi.org/10.1002/ajmg.b.10024.
- 3 Sullivan PF, Kendler KS, Neale MC. Schizophrenia as a complex trait: evidence from a metaanalysis of twin studies. *Arch Gen Psychiatry* 2003;**60**:1187–92. https://doi.org/10.1001/archpsyc.60.12.1187.
- 4 Sandin S, Lichtenstein P, Kuja-Halkola R, Hultman C, Larsson H, Reichenberg A. The Heritability of Autism Spectrum Disorder. *JAMA* 2017;**318**:1182–4. https://doi.org/10.1001/jama.2017.12141.
- 5 Ng MYM, Levinson DF, Faraone SV, Suarez BK, DeLisi LE, Arinami T, *et al.* Meta-analysis of 32 genome-wide linkage studies of schizophrenia. *Mol Psychiatry* 2009;**14**:774–85. https://doi.org/10.1038/mp.2008.135.
- 6 Ottman R. Gene-environment interaction: definitions and study designs. *Prev Med* 1996;**25**:764–70.
- 7 Duncan LE, Keller MC. A critical review of the first 10 years of candidate gene-by-environment interaction research in psychiatry. *Am J Psychiatry* 2011;**168**:1041–9. https://doi.org/10.1176/appi.ajp.2011.11020191.

- 8 Schizophrenia Working Group of the Psychiatric Genomics Consortium. Biological insights from 108 schizophrenia-associated genetic loci. *Nature* 2014;**511**:421–7. https://doi.org/10.1038/nature13595.
- 9 Coe BP, Girirajan S, Eichler EE. The genetic variability and commonality of neurodevelopmental disease. Am J Med Genet C Semin Med Genet 2012;160C:118–29. https://doi.org/10.1002/ajmg.c.31327.
- 10Malhotra D, Sebat J. CNVs: Harbinger of a Rare Variant Revolution in Psychiatric Genetics.

 *Cell 2012;148:1223–41. https://doi.org/10.1016/j.cell.2012.02.039.
- 11Girirajan S, Rosenfeld JA, Coe BP, Parikh S, Friedman N, Goldstein A, *et al.* Phenotypic Heterogeneity of Genomic Disorders and Rare Copy-Number Variants. *N Engl J Med* 2012;**367**:1321–31. https://doi.org/10.1056/NEJMoa1200395.
- 12De Leersnyder H. Chapter 34 Smith–Magenis syndrome. In: Dulac O, Lassonde M, Sarnat HB, editors. *Handb. Clin. Neurol.*, vol. 111. Elsevier; 2013. p. 295–6.
- 13Goodship J, Cross I, LiLing J, Wren C. A population study of chromosome 22q11 deletions in infancy. *Arch Dis Child* 1998;**79**:348–51. https://doi.org/10.1136/adc.79.4.348.
- 14McDonald-McGinn DM, Sullivan KE, Marino B, Philip N, Swillen A, Vorstman JAS, et al.22q11.2 deletion syndrome. Nat Rev Dis Primer 2015;1:15071.https://doi.org/10.1038/nrdp.2015.71.
- 15 Psychosis Endophenotypes International Consortium, CNV and Schizophrenia Working

 Groups of the Psychiatric Genomics Consortium, Marshall CR, Howrigan DP, Merico D,

 Thiruvahindrapuram B, et al. Contribution of copy number variants to schizophrenia from a

- genome-wide study of 41,321 subjects. *Nat Genet* 2017;**49**:27–35. https://doi.org/10.1038/ng.3725.
- 16Mulle JG. The 3q29 deletion confers >40-fold increase in risk for schizophrenia. *Mol Psychiatry* 2015;**20**:1028–9. https://doi.org/10.1038/mp.2015.76.
- 17Cox DM, Butler MG. A clinical case report and literature review of the 3q29 microdeletion syndrome: *Clin Dysmorphol* 2015;**24**:89–94. https://doi.org/10.1097/MCD.0000000000000077.
- 18Stefansson H, Meyer-Lindenberg A, Steinberg S, Magnusdottir B, Morgen K, Arnarsdottir S, *et al.* CNVs conferring risk of autism or schizophrenia affect cognition in controls. *Nature* 2014;**505**:361–6. https://doi.org/10.1038/nature12818.
- 19 Glassford MR, Rosenfeld JA, Freedman AA, Zwick ME, Unique Rare Chromosome Disorder Support Group, Mulle JG. Novel features of 3q29 deletion syndrome: Results from the 3q29 registry: Novel Features of 3q29 Deletion Syndrome. *Am J Med Genet A* 2016;**170**:999–1006. https://doi.org/10.1002/ajmg.a.37537.
- 20Willatt L, Cox J, Barber J, Cabanas ED, Collins A, Donnai D, *et al.* 3q29 Microdeletion Syndrome: Clinical and Molecular Characterization of a New Syndrome. *Am J Hum Genet* 2005;**77**:154–60. https://doi.org/10.1086/431653.
- 21Sanders SJ, He X, Willsey AJ, Ercan-Sencicek AG, Samocha KE, Cicek AE, *et al.* Insights into Autism Spectrum Disorder Genomic Architecture and Biology from 71 Risk Loci. *Neuron* 2015;**87**:1215–33. https://doi.org/10.1016/j.neuron.2015.09.016.
- 22 Ballif BC, Theisen A, Coppinger J, Gowans GC, Hersh JH, Madan-Khetarpal S, et al. Expanding the clinical phenotype of the 3q29 microdeletion syndrome and characterization of the

- reciprocal microduplication. *Mol Cytogenet* 2008;**1**:8. https://doi.org/10.1186/1755-8166-1-8.
- 23Murphy MM, Lindsey Burrell T, Cubells JF, España RA, Gambello MJ, Goines KCB, *et al.* Study protocol for The Emory 3q29 Project: evaluation of neurodevelopmental, psychiatric, and medical symptoms in 3q29 deletion syndrome. *BMC Psychiatry* 2018;**18**:183. https://doi.org/10.1186/s12888-018-1760-5.
- 24Rutkowski TP, Purcell RH, Pollak RM, Grewenow SM, Gafford GM, Malone T, *et al.* Behavioral changes and growth deficits in a CRISPR engineered mouse model of the schizophrenia-associated 3q29 deletion. *Mol Psychiatry* 2019. https://doi.org/10.1038/s41380-019-0413-5.
- 25 Hawrylycz MJ, Lein ES, Guillozet-Bongaarts AL, Shen EH, Ng L, Miller JA, *et al.* An anatomically comprehensive atlas of the adult human brain transcriptome. *Nature* 2012;**489**:391–9. https://doi.org/10.1038/nature11405.
- 26Quintero-Rivera F, Sharifi-Hannauer P, Martinez-Agosto JA. Autistic and psychiatric findings associated with the 3q29 microdeletion syndrome: Case report and review. *Am J Med Genet A* 2010;**152A**:2459–67. https://doi.org/10.1002/ajmg.a.33573.
- 27Tada H, Okano HJ, Takagi H, Shibata S, Yao I, Matsumoto M, *et al.* Fbxo45, a Novel Ubiquitin Ligase, Regulates Synaptic Activity. *J Biol Chem* 2010;**285**:3840–9. https://doi.org/10.1074/jbc.M109.046284.
- 28Bokoch GM. Biology of the p21-activated kinases. *Annu Rev Biochem* 2003;**72**:743–81. https://doi.org/10.1146/annurev.biochem.72.121801.161742.

- 29Wang Y, Zeng C, Li J, Zhou Z, Ju X, Xia S, *et al.* PAK2 Haploinsufficiency Results in Synaptic Cytoskeleton Impairment and Autism-Related Behavior. *Cell Rep* 2018;**24**:2029–41. https://doi.org/10.1016/j.celrep.2018.07.061.
- 30Rutkowski TP, Schroeder JP, Gafford GM, Warren ST, Weinshenker D, Caspary T, et al.

 Unraveling the genetic architecture of copy number variants associated with schizophrenia and other neuropsychiatric disorders: CNVs in Neuropsychiatric Disorders. *J Neurosci Res*2017;**95**:1144–60. https://doi.org/10.1002/jnr.23970.
- 31Toyooka K, Iritani S, Makifuchi T, Shirakawa O, Kitamura N, Maeda K, *et al.* Selective reduction of a PDZ protein, SAP-97, in the prefrontal cortex of patients with chronic schizophrenia: PDZ molecules in schizophrenic brain. *J Neurochem* 2002;**83**:797–806. https://doi.org/10.1046/j.1471-4159.2002.01181.x.
- 32 Purcell SM, Moran JL, Fromer M, Ruderfer D, Solovieff N, Roussos P, et al. A polygenic burden of rare disruptive mutations in schizophrenia. *Nature* 2014;**506**:185–90. https://doi.org/10.1038/nature12975.
- 33 Gupta P, Uner OE, Nayak S, Grant GR, Kalb RG. SAP97 regulates behavior and expression of schizophrenia risk enriched gene sets in mouse hippocampus. *PloS One* 2018;**13**:e0200477. https://doi.org/10.1371/journal.pone.0200477.
- 34Grice SJ, Liu J-L, Webber C. Synergistic Interactions between Drosophila Orthologues of Genes Spanned by De Novo Human CNVs Support Multiple-Hit Models of Autism. *PLOS Genet* 2015;**11**:e1004998. https://doi.org/10.1371/journal.pgen.1004998.

- 35Singh MD, Jensen M, Lasser M, Huber E, Yusuff T, Pizzo L, *et al.* NCBP2-mediated apoptosis contributes to developmental defects of the schizophrenia-associated 3q29 deletion. *BioRxiv* 2019:614750. https://doi.org/10.1101/614750.
- 36Lewandoski M, Martin GR. Cre-mediated chromosome loss in mice. *Nat Genet* 1997;**17**:223–5. https://doi.org/10.1038/ng1097-223.
- 37Lindsay EA, Botta A, Jurecic V, Carattini-Rivera S, Cheah YC, Rosenblatt HM, et al. Congenital heart disease in mice deficient for the DiGeorge syndrome region. *Nature* 1999;**401**:379–83. https://doi.org/10.1038/43900.
- 38Yu YE, Morishima M, Pao A, Wang D-Y, Wen X-Y, Baldini A, *et al.* A Deficiency in the Region Homologous to Human 17q21.33–q23.2 Causes Heart Defects in Mice. *Genetics* 2006;**173**:297–307. https://doi.org/10.1534/genetics.105.054833.
- 39Yu T, Clapcote SJ, Li Z, Liu C, Pao A, Bechard AR, *et al.* Deficiencies in the region syntenic to human 21q22.3 cause cognitive deficits in mice. *Mamm Genome Off J Int Mamm Genome Soc* 2010;**21**:258–67. https://doi.org/10.1007/s00335-010-9262-x.
- 40Sonoda E, Hochegger H, Saberi A, Taniguchi Y, Takeda S. Differential usage of non-homologous end-joining and homologous recombination in double strand break repair. *DNA Repair* 2006;**5**:1021–9. https://doi.org/10.1016/j.dnarep.2006.05.022.
- 41Hsu PD, Scott DA, Weinstein JA, Ran FA, Konermann S, Agarwala V, et al. DNA targeting specificity of RNA-guided Cas9 nucleases. *Nat Biotechnol* 2013;**31**:827–32. https://doi.org/10.1038/nbt.2647.
- 42Cong L, Ran FA, Cox D, Lin S, Barretto R, Habib N, et al. Multiplex genome engineering using CRISPR/Cas systems. *Science* 2013;**339**:819–23. https://doi.org/10.1126/science.1231143.

- 43 Forsingdal A, Fejgin K, Nielsen V, Werge T, Nielsen J. 15q13.3 homozygous knockout mouse model display epilepsy-, autism- and schizophrenia-related phenotypes. *Transl Psychiatry* 2016;**6**:e860. https://doi.org/10.1038/tp.2016.125.
- 44Uddin M, Unda BK, Kwan V, Holzapfel NT, White SH, Chalil L, *et al.* OTUD7A Regulates

 Neurodevelopmental Phenotypes in the 15q13.3 Microdeletion Syndrome. *Am J Hum Genet*2018;**102**:278–95. https://doi.org/10.1016/j.ajhg.2018.01.006.
- 45 Escamilla CO, Filonova I, Walker AK, Xuan ZX, Holehonnur R, Espinosa F, et al. Kctd13 deletion reduces synaptic transmission via increased RhoA. Nature 2017;**551**:227–31. https://doi.org/10.1038/nature24470.
- 46Richter M, Murtaza N, Scharrenberg R, White SH, Johanns O, Walker S, *et al.* Altered TAOK2 activity causes autism-related neurodevelopmental and cognitive abnormalities through RhoA signaling. *Mol Psychiatry* 2018:1. https://doi.org/10.1038/s41380-018-0025-5.
- 47 Pucilowska J, Vithayathil J, Tavares EJ, Kelly C, Karlo JC, Landreth GE. The 16p11.2 Deletion Mouse Model of Autism Exhibits Altered Cortical Progenitor Proliferation and Brain Cytoarchitecture Linked to the ERK MAPK Pathway. *J Neurosci* 2015;**35**:3190–200. https://doi.org/10.1523/JNEUROSCI.4864-13.2015.
- 48 Horev G, Ellegood J, Lerch JP, Son Y-EE, Muthuswamy L, Vogel H, *et al.* Dosage-dependent phenotypes in models of 16p11.2 lesions found in autism. *Proc Natl Acad Sci* 2011;**108**:17076–81. https://doi.org/10.1073/pnas.1114042108.
- 49Edelmann L, Pandita RK, Morrow BE. Low-copy repeats mediate the common 3-Mb deletion in patients with velo-cardio-facial syndrome. *Am J Hum Genet* 1999;**64**:1076–86.

- 50Antonacci F, Kidd JM, Marques-Bonet T, Ventura M, Siswara P, Jiang Z, et al. Characterization of six human disease-associated inversion polymorphisms. *Hum Mol Genet* 2009;**18**:2555–66. https://doi.org/10.1093/hmg/ddp187.
- 51Xie N, Gong H, Suhl JA, Chopra P, Wang T, Warren ST. Reactivation of FMR1 by CRISPR/Cas9-Mediated Deletion of the Expanded CGG-Repeat of the Fragile X Chromosome. *PloS One* 2016;**11**:e0165499. https://doi.org/10.1371/journal.pone.0165499.
- 52Yang M, Silverman JL, Crawley JN. Automated three-chambered social approach task for mice. *Curr Protoc Neurosci* 2011; Chapter 8:Unit 8.26. https://doi.org/10.1002/0471142301.ns0826s56.
- 53Zhang J-H, Adikaram P, Pandey M, Genis A, Simonds WF. Optimization of genome editing through CRISPR-Cas9 engineering. *Bioengineered* 2016;**7**:166–74. https://doi.org/10.1080/21655979.2016.1189039.
- 54Sittig LJ, Carbonetto P, Engel KA, Krauss KS, Barrios-Camacho CM, Palmer AA. Genetic Background Limits Generalizability of Genotype-Phenotype Relationships. *Neuron* 2016;**91**:1253–9. https://doi.org/10.1016/j.neuron.2016.08.013.
- 55 Williams MR, Chaudhry R, Perera S, Pearce RKB, Hirsch SR, Ansorge O, *et al.* Changes in cortical thickness in the frontal lobes in schizophrenia are a result of thinning of pyramidal cell layers. *Eur Arch Psychiatry Clin Neurosci* 2013;**263**:25–39. https://doi.org/10.1007/s00406-012-0325-8.
- 56Hevner RF, Shi L, Justice N, Hsueh Y-P, Sheng M, Smiga S, et al. Tbr1 Regulates Differentiation of the Preplate and Layer 6. *Neuron* 2001;**29**:353–66. https://doi.org/10.1016/S0896-6273(01)00211-2.

- 57 Baba M, Yokoyama K, Seiriki K, Naka Y, Matsumura K, Kondo M, *et al.* Psychiatric-disorder-related behavioral phenotypes and cortical hyperactivity in a mouse model of 3q29 deletion syndrome. *Neuropsychopharmacology* 2019:1. https://doi.org/10.1038/s41386-019-0441-5. 58 Cooper GM. The Eukaryotic Cell Cycle. *Cell Mol Approach 2nd Ed* 2000.
- 59Cam H, Balciunaite E, Blais A, Spektor A, Scarpulla RC, Young R, et al. A Common Set of Gene Regulatory Networks Links Metabolism and Growth Inhibition. *Mol Cell* 2004;**16**:399–411. https://doi.org/10.1016/j.molcel.2004.09.037.
- 60Fombonne E. Epidemiology of pervasive developmental disorders. *Pediatr Res* 2009;**65**:591–8. https://doi.org/10.1203/PDR.0b013e31819e7203.
- 61Takahashi A, Nishi A, Ishii A, Shiroishi T, Koide T. Systematic analysis of emotionality in consomic mouse strains established from C57BL/6J and wild-derived MSM/Ms. *Genes Brain Behav* 2008;**7**:849–58. https://doi.org/10.1111/j.1601-183X.2008.00419.x.
- 62 Caviness VS, Takahashi T, Nowakowski RS. Numbers, time and neocortical neuronogenesis: a general developmental and evolutionary model. *Trends Neurosci* 1995;**18**:379–83. https://doi.org/10.1016/0166-2236(95)93933-O.
- 63 Lupiáñez DG, Spielmann M, Mundlos S. Breaking TADs: How Alterations of Chromatin Domains Result in Disease. *Trends Genet* 2016;**32**:225–37. https://doi.org/10.1016/j.tig.2016.01.003.
- 64Slavotinek A, Biesecker LG. Genetic modifiers in human development and malformation syndromes, including chaperone proteins. *Hum Mol Genet* 2003;**12 Spec No 1**:R45-50. https://doi.org/10.1093/hmg/ddg099.

- 65 Noubade R, Wong K, Ota N, Rutz S, Eidenschenk C, Valdez PA, et al. NRROS negatively regulates reactive oxygen species during host defence and autoimmunity. *Nature* 2014;**509**:235–9. https://doi.org/10.1038/nature13152.
- 66Wong K, Noubade R, Manzanillo P, Ota N, Foreman O, Hackney JA, et al. Mice deficient in NRROS show abnormal microglial development and neurological disorders. *Nat Immunol* 2017;**18**:633–41. https://doi.org/10.1038/ni.3743.
- 67 Wang L, Magdaleno S, Tabas I, Jackowski S. Early Embryonic Lethality in Mice with Targeted Deletion of the CTP:Phosphocholine Cytidylyltransferase α Gene (Pcyt1a). *Mol Cell Biol* 2005;**25**:3357–63. https://doi.org/10.1128/MCB.25.8.3357-3363.2005.
- 68 Newman JC, Verdin E. β-hydroxybutyrate: Much more than a metabolite. *Diabetes Res Clin Pract* 2014;**106**:173–81. https://doi.org/10.1016/j.diabres.2014.08.009.
- 69Horton JL, Davidson MT, Kurishima C, Vega RB, Powers JC, Matsuura TR, et al. The failing heart utilizes 3-hydroxybutyrate as a metabolic stress defense. *JCI Insight* n.d.;**4**:. https://doi.org/10.1172/jci.insight.124079.
- 70Zunino R, Schauss A, Rippstein P, Andrade-Navarro M, McBride HM. The SUMO protease SENP5 is required to maintain mitochondrial morphology and function. *J Cell Sci* 2007;**120**:1178–88. https://doi.org/10.1242/jcs.03418.
- 71Kim EY, Zhang Y, Beketaev I, Segura AM, Yu W, Xi Y, *et al.* SENP5, a SUMO isopeptidase, induces apoptosis and cardiomyopathy. *J Mol Cell Cardiol* 2015;**78**:154–64. https://doi.org/10.1016/j.yjmcc.2014.08.003.

- 72 Bacco AD, Ouyang J, Lee H-Y, Catic A, Ploegh H, Gill G. The SUMO-Specific Protease SENP5 Is

 Required for Cell Division. *Mol Cell Biol* 2006;**26**:4489–98.

 https://doi.org/10.1128/MCB.02301-05.
- 73The International Mouse Phenotyping Consortium, Dickinson ME, Flenniken AM, Ji X, Teboul L, Wong MD, *et al.* High-throughput discovery of novel developmental phenotypes. *Nature* 2016;**537**:508–14. https://doi.org/10.1038/nature19356.
- 74Senyilmaz D, Virtue S, Xu X, Tan CY, Griffin JL, Miller AK, et al. Regulation of mitochondrial morphology and function by stearoylation of TFR1. *Nature* 2015;**525**:124–8. https://doi.org/10.1038/nature14601.
- 75 Levy JE, Jin O, Fujiwara Y, Kuo F, Andrews N. Transferrin receptor is necessary for development of erythrocytes and the nervous system. *Nat Genet* 1999;**21**:396. https://doi.org/10.1038/7727.
- 76 Dunn LL, Sekyere EO, Suryo Rahmanto Y, Richardson DR. The function of melanotransferrin: a role in melanoma cell proliferation and tumorigenesis. *Carcinogenesis* 2006;**27**:2157–69. https://doi.org/10.1093/carcin/bgl045.
- 77Suryo Rahmanto Y, Dunn LL, Richardson DR. The melanoma tumor antigen,
 melanotransferrin (p97): a 25-year hallmark from iron metabolism to tumorigenesis.

 Oncogene 2007;26:6113–24. https://doi.org/10.1038/sj.onc.1210442.
- 78Stewart GS, Panier S, Townsend K, Al-Hakim AK, Kolas NK, Miller ES, et al. The RIDDLE Syndrome Protein Mediates a Ubiquitin-Dependent Signaling Cascade at Sites of DNA Damage. *Cell* 2009;**136**:420–34. https://doi.org/10.1016/j.cell.2008.12.042.

- 79Bohgaki T, Bohgaki M, Cardoso R, Panier S, Zeegers D, Li L, *et al.* Genomic Instability,

 Defective Spermatogenesis, Immunodeficiency, and Cancer in a Mouse Model of the RIDDLE

 Syndrome. *PLoS Genet* 2011;**7**:. https://doi.org/10.1371/journal.pgen.1001381.
- 80Bandau S, Knebel A, Gage ZO, Wood NT, Alexandru G. UBXN7 docks on neddylated cullin complexes using its UIM motif and causes HIF1α accumulation. *BMC Biol* 2012;**10**:36. https://doi.org/10.1186/1741-7007-10-36.
- 81 Higa LA, Wu M, Ye T, Kobayashi R, Sun H, Zhang H. CUL4-DDB1 ubiquitin ligase interacts with multiple WD40-repeat proteins and regulates histone methylation. *Nat Cell Biol* 2006;**8**:1277–83. https://doi.org/10.1038/ncb1490.
- 82Yıldız Bölükbaşı E, Mumtaz S, Afzal M, Woehlbier U, Malik S, Tolun A. Homozygous mutation in CEP19, a gene mutated in morbid obesity, in Bardet-Biedl syndrome with predominant postaxial polydactyly. *J Med Genet* 2018;**55**:189–97. https://doi.org/10.1136/jmedgenet-2017-104758.
- 83 Nishijima Y, Hagiya Y, Kubo T, Takei R, Katoh Y, Nakayama K. RABL2 interacts with the intraflagellar transport-B complex and CEP19 and participates in ciliary assembly. *Mol Biol Cell* 2017;**28**:1652–66. https://doi.org/10.1091/mbc.E17-01-0017.
- 84Shalata A, Ramirez MC, Desnick RJ, Priedigkeit N, Buettner C, Lindtner C, et al. Morbid

 Obesity Resulting from Inactivation of the Ciliary Protein CEP19 in Humans and Mice. Am J

 Hum Genet 2013;93:1061–71. https://doi.org/10.1016/j.ajhg.2013.10.025.